Macroscopic deformation modes of origami tessellations and periodic pin-jointed trusses: the case of the eggbox

Hussein Nassar, Arthur Lebée, Laurent Monasse

September 25th - 28th, 2017
INTERFACES
architecture . engineering . science IASS 2017 hamburg

Proceedings of the IASS Annual Symposium 2017
"Interfaces: architecture.engineering.science"
25 - 28th September, 2017, Hamburg, Germany
Annette Bögle, Manfred Grohmann (eds.)

Macroscopic deformation modes of origami tessellations and periodic pin-jointed trusses: the case of the eggbox

Hussein NASSAR[a,b], Arthur LEBÉE[a,]*, Laurent MONASSE[b]

*arthur.lebee@enpc.fr

[a] Laboratoire Navier, Ecole des Ponts-ParisTech, IFSTTAR, CNRS, UPE, 6 et 8 Avenue Blaise Pascal, 77455 Marne-la-Vallée cedex 2
[b] Université Paris-Est, Cermics (ENPC), INRIA, F-77455 Marne-la-Vallée

Abstract

Origami tessellations are particular textured morphing shell structures. Their unique folding and unfolding mechanisms at a local scale aggregate and bring on large changes in shape, curvature and elongation at a global scale. The existence of these global deformation modes allows for origami tessellations to fit non-trivial surfaces. This paper characterizes the parametrization, curvature and metric of smooth surfaces that the eggbox pattern can fit asymptotically, i.e., when the eggbox unit cell parameter becomes infinitely small compared to the typical radius of curvature of the target surface. In particular, it is demonstrated that no finite region of a sphere can be fitted and a systematic method that allows to fit ruled surfaces is presented. As an application, the fitting of a one-sheeted hyperboloid is constructed.

Keywords: Origami, metasurface, form finding, floppy modes, eggbox.

1. Introduction

Structured materials inspired from the art of paper folding, Origami, have proven useful in various fields spanning architecture, structural, aerospace and biomedical engineering as well as elastic and acoustic wave motion and control (see, e.g., Hochfeld [6], Miura [7] and Resch and Christiansen [9]). Origami tessellations in particular offer numerous possibilities for the design of morphing shell structures. Their intricate folding and unfolding mechanisms are organized on both local and global scales and are capable of bringing on large deformations and considerable changes in shape, curvature and elongation. These global deformation modes allow origami tessellations to fit non-trivial curved surfaces even when they are made of an inextensible material, such as paper.

When no folds are allowed, Euler [3] proved early that paper may only fit developable surfaces. The case of weavings as well as gridshells was investigated by Chebyshev [2,4]. Falling out of these contexts, origami tessellations require a specific analysis on their own. In the present work, we suggest an upscaling method which yields a macroscopic continuous description of the global deformation modes of a given origami tessellation fully detailed by the authors in reference [8]. The method characterizes the parametrization, metric and curvature of smooth surfaces that the discrete structure can fit. The theory is presented through a case study of a fairly generic example: the eggbox pattern (Schenk [10]). The proposed continuous model successfully predicts the existence of various fittings featuring large and finite changes in metric and curvature. In particular, we prove that the eggbox cannot fit any finite region of a sphere and present a systematic method that allows to fit any ruled surface.

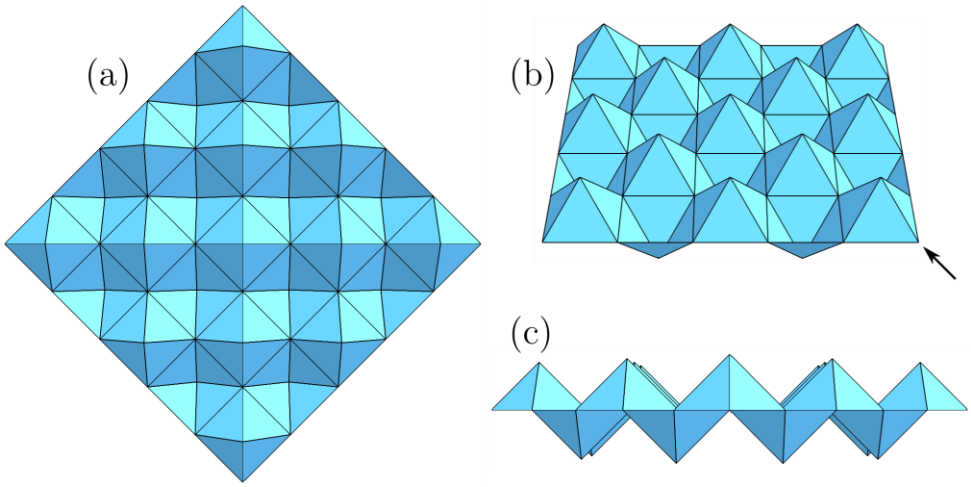

Figure 1: An eggbox in its reference state: (a) top view, (b) isometric view, (c) corner side view as indicated by the arrow.

2. The eggbox as a discrete structure

The eggbox is a pyramidal truss where the orientation of the pyramids is alternated in a checkerboard pattern (Figure 1). Vertices are assumed to behave like pivots whereas edges are taken to be rigid. Though not an origami strictly speaking, the eggbox can be described by the same spherical joints mechanisms that govern origami. In that picture, facets are considered to be made of an inextensible material such as paper and edges are freely rotating hinges modeling creases. For our purposes, the truss model will prove more useful and is adopted in what follows. Also, for simplicity, we take all pyramids to be initially square-based with equilateral lateral facets. As a consequence, all edges are identical and keep a constant length r.

2.1. One pyramid

Before tackling complex constructs, it is wise to describe the elementary mechanism governing a single pyramid. Looking at Figure 2, it is seen that the position of the bipod (u, v) controls unambiguously, up to orientation, the position of the whole pyramid. While u and v must be of length r, the unique deformation parameter at play is the angle θ given by $\cos\theta = \langle u, v\rangle / r^2$, $\theta \in [0,2\pi/3]$. Let us also define w and w^*as the vectors initially placed on the diagonals of the pyramid basis and moving with the vertices in any subsequent motion. Clearly, $w = u - v$ whereas $w^* = w^*(u, v)$ has a more complex expression that should not interest us here. Together with the pyramid's apex, w and w^* form two isosceles triangles of heights $r\sqrt{1 - s^2}$ and $r\sqrt{1 - s^{*2}}$, respectively, where $2rs$ and $2rs^*$ are the respective magnitudes of w and w^*. Due to mirror symmetry, these two triangles belong to two orthogonal planes. Thus, injecting the apex of the pyramid into the dot product $\langle w, w^*\rangle = 0$ using Chasles' relation readily implies the identity

$$4(1 - s^2)(1 - s^{*2}) = 1.$$

Here too, due to our favoring one side over the other in choosing u and v, s admits a simple expression in terms of θ, namely $s = \sin(\theta/2)$, but s^* does not and needs to be deduced from the previous identity relating s and s^*. In any case, we see that as s increases, s^* decreases and both remain comprised between 0 and $\sqrt{3}/2$.

Concluding these preliminaries, a pyramid can be described, we say parametrized, by the giving of either one of the bipods (u, v) or (w, w^*). In case the latter is adopted, one needs to be careful choosing

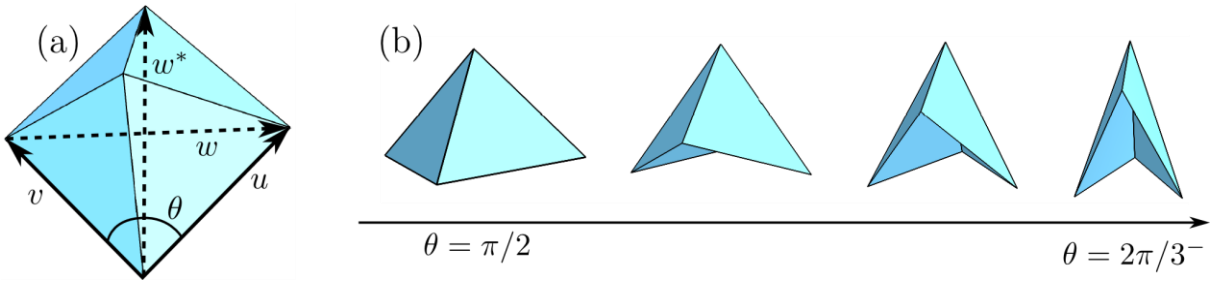

Figure 2: A pyramid: (a) notations, (b) unique deformation mode.

compatible vectors w and w^* by making sure that they satisfy both necessary conditions given above, i.e., orthogonality and magnitude identity.

2.2. $N \times N$ pyramids

Now consider an eggbox composed initially of a square of $N \times N$ pyramids and consider the pyramids laying at one of its diagonals, say the one with positively oriented pyramids, called D_0 (Figure 3). On D_0, pyramid number m is parametrized by a bipod $(u_{m,0}, v_{m,0})$ and given the series of bipods $(u_{m,0}, v_{m,0})$, $m = 1 \dots N$, one should be able to reconstruct the whole diagonal D_0. In doing so, one would have constructed the bipods $(u_{m,1}, v_{m,1})$, $m = 1 \dots N - 1$, of the next diagonal D_1. Hence, it is possible to construct all pyramids located on D_1. By iterating this process, in both directions, and alternating the orientation of the pyramids at each step, all bipods $(u_{m,n}, v_{m,n})$ can be constructed.

In conclusion, an $N \times N$ eggbox is uniquely parametrized by a series of N bipods $(u_{m,0}, v_{m,0})$ laying at its principal diagonal. That is, the motion of the principal diagonal determines unambiguously the motion of the whole eggbox. Note that we do not claim that any motion of the diagonal will be compatible with all of the geometric constraints within the eggbox but only that, in case it is, the dictated motion of the eggbox will be unique and unambiguous. In other words, an $N \times N$ eggbox has at most $4N + 3$ degrees of freedom. Finally, though it might be harder to visualize, we insist on the fact that it is equivalent to use the bipods $(w_{m,0}, w^*_{m,0})$ to parametrize the motion of the same eggbox.

This algorithm was implemented in the language Python (libraries numpy and mayavi) and used to generate the 3D plots of this paper.

3. The eggbox as a smooth surface

3.1. Periodicity and scale invariance

We say that the eggbox is periodic in the sense that it has a reference configuration that is invariant by two independent translations, w and w^*. Integer combinations of w and w^* will be referred to as lattice vectors. Note that the eggbox is not invariant by translation along u and v.

Here, it is worth mentioning that the construction algorithm we described in the previous section still works even if the eggbox was not periodic, i.e., even if some of the pyramids were distorted. In contrast, the considerations of this section are deeply rooted in the periodicity assumption.

In what follows, our aim is to describe the smooth surfaces that an eggbox can fit in the limit $r \to 0$. It is not clear however what that limit corresponds to physically since the eggbox has scale-invariant kinematics: if V is a set of points that can be occupied by the vertices of an eggbox of edge size r then αV is a set of points that can be occupied by the vertices of an eggbox of edge size αr, $\alpha > 0$. This means that the eggbox has no internal characteristic length scale compared to which r will be infinitely small. Luckily, the target smooth surface typical radius of curvature R still provides an external characteristic length scale and the limit $r \to 0$ is to be understood as $r/R \ll 1$.

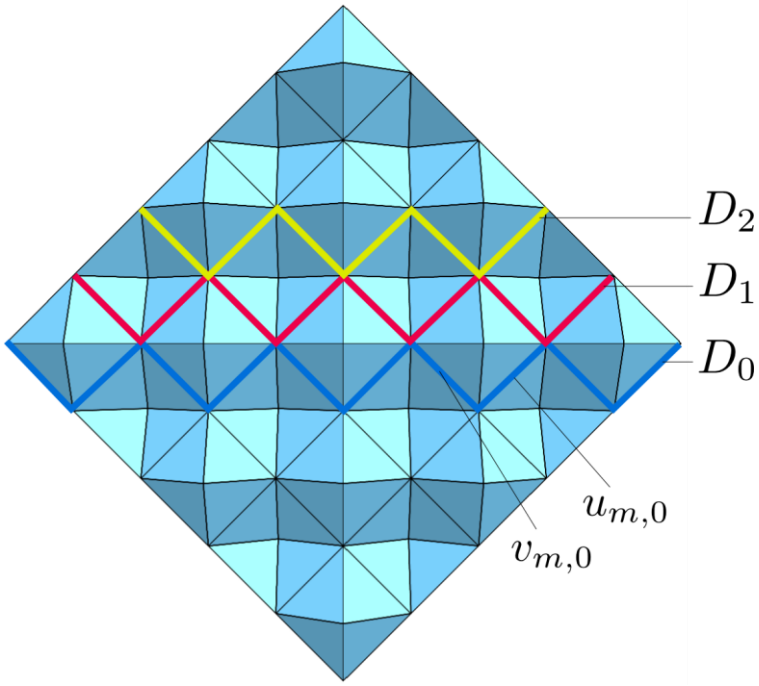

Figure 3: Illustration of the construction algorithm: given D_0, D_1 is uniquely determined.

3.2. Parametrization

Let S be a smooth surface that the eggbox asymptotically fits. We describe this surface through a parametrization $\phi\colon \mathbb{R}^2 \to S \subset \mathbb{R}^3$ so that when (x, y) moves through $\mathbb{R}^2$, $\phi(x, y)$ moves through S. With no loss of generality, we let x and y respectively be the coordinates along w and w^*in the reference configuration.

Derivatives of ϕ in the x and y directions, called ϕ_x and ϕ_y, yield tangent vectors to S and their scalar products define the metric, also called the first fundamental form, of S:

$$I = \begin{bmatrix} \langle \phi_x, \phi_x \rangle & \langle \phi_x, \phi_y \rangle \\ \langle \phi_x, \phi_y \rangle & \langle \phi_y, \phi_y \rangle \end{bmatrix}.$$

Their normalized cross product, $\hat{n}$, is then normal to S and allows to define the second fundamental form

$$II = \begin{bmatrix} L & M \\ M & N \end{bmatrix} = \begin{bmatrix} \langle \phi_{xx}, \hat{n} \rangle & \langle \phi_{xy}, \hat{n} \rangle \\ \langle \phi_{xy}, \hat{n} \rangle & \langle \phi_{yy}, \hat{n} \rangle \end{bmatrix}.$$

The curvatures in the directions x and y are then given by

$$\kappa_1 = L/\|\phi_x\|^2, \qquad \kappa_2 = N/\|\phi_y\|^2.$$

See Ciarlet [1] for more details and for an introduction to the differential geometry of surfaces.

The fact that S can be asymptotically fitted by an eggbox yields a couple of identities that the forms I and II must satisfy and are presented next.

3.3. Convergence

Before going any further, we need to agree on a definition of the convergence process. A poor definition of convergence is to require that the vertices of the eggbox indefinitely approach the points of S. Here, we demand much more: that equal lattice vectors converge to equal tangent vectors and that differences

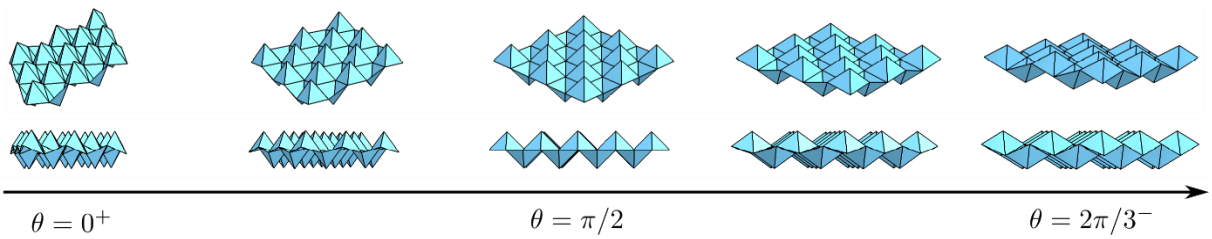

Figure 4: Flat-folding motion of the eggbox.

between lattice vectors converge to derivatives of tangent vectors. This amounts to stating that as the eggbox fits S asymptotically, it also fits its tangent planes and its osculating parabolas.

More precisely, let P be a point of S of coordinates (x, y). Then, let $w_{m,n}(x, y)$ and $w^*_{m,n}(x, y)$ designate all lattice vectors of the fitting that are in a neighborhood ν of radius ρ centered on P. As r goes to 0, it is possible to choose ρ such that $r \ll \rho \ll R$ so that ν contains a significant number of pyramids of order $N \times N$ with N comparable to ρ/r. Then, regarding first order derivatives, we have

$$w_{m,n}(x, y) = r\phi_x(x, y) + o(r), \qquad w^*_{m,n}(x, y) = r\phi_y(x, y) + o(r).$$

Therefore, the $N \times N$ pyramids in the vicinity of P are, to leading order in r, in a periodic configuration since all vectors $w_{m,n}(x, y)$ (respectively $w^*_{m,n}(x, y)$) are equal to one another and to $r\phi_x(x, y)$ (respectively $r\phi_y(x, y)$). It turns out that the eggbox admits such periodic configurations (other than its reference one). They are illustrated on Figure 4 and describe a flat-folding motion of the eggbox. Each periodic configuration is uniquely designated by the folding angle θ which is the same for all the pyramids. These periodic states can be constructed by initiating our construction algorithm with $w_{m,0} = r\phi_x(x, y)$ and $w^*_{m,0} = r\phi_y(x, y)$, $m = 1 \dots N$. In conclusion, the folding angle $\theta(x, y)$ at P can be unambiguously defined through $\|\phi_x\| = 2s = 2\sin(\theta/2)$. We then also deduce that

$$I = \begin{bmatrix} 4s^2 & 0 \\ 0 & 4s^{*2} \end{bmatrix},$$

where dependence on (x, y) has been dropped.

Regarding second order derivatives, convergence requires

$$\begin{aligned} w_{m+1,n}(x, y) - w_{m,n}(x, y) &= r^2\phi_{xx}(x, y) + o(r^2), \\ w^*_{m,n+1}(x, y) - w^*_{m,n}(x, y) &= r^2\phi_{yy}(x, y) + o(r^2), \\ w_{m,n+1}(x, y) - w_{m,n}(x, y) &= r^2\phi_{xy}(x, y) + o(r^2). \end{aligned}$$

It appears then that the periodic states of the eggbox are being infinitesimally perturbed. This perturbation is not arbitrary but rather uniform across the $N \times N$ pyramids. Yet our construction algorithm informs us that it is enough to know how the principal diagonal is perturbed to determine how the whole structure changes implying that ϕ_{xx}, ϕ_{yy} and ϕ_{xy} must satisfy some compatibility relation. Starting with an arbitrary periodic state and adding a uniform infinitesimal perturbation, it can be concluded that this compatibility relation is

$$\frac{L}{1 - s^2} = \frac{N}{1 - s^{*2}}.$$

See Nassar *et al.* [8] for more details.

3.4. The fitting problem

We are now ready to formulate the fitting problem on the macroscopic scale.

Let S be a smooth surface that can be asymptotically fitted by an eggbox. Then there exists a parametrization ϕ in which the first and second fundamental forms of S read

$$I = \begin{bmatrix} 4s^2 & 0 \\ 0 & 4s^{*2} \end{bmatrix}, \qquad II = \begin{bmatrix} L & M \\ M & N \end{bmatrix},$$

with

$$s, s^* \in]0, \sqrt{3}/2[, \qquad 4(1-s^2)(1-s^{*2}) = 1, \qquad \frac{L}{1-s^2} = \frac{N}{1-s^{*2}}. \quad (*)$$

In particular, using the frame equations, it is deduced that ϕ must satisfy the nonlinear vector wave equation

$$\frac{\phi_{xx}}{1-s^2} - \frac{\phi_{yy}}{1-s^{*2}} = 0$$

where, say, x plays the role of space and y the role of time. This result is the continuous version of our construction algorithm: by prescribing the "initial data" $\phi_x(x,0)$ and $\phi_y(x,0)$, a unique fitting can be constructed by solving the above motion equation with an iterative scheme for instance.

Once a fitting ϕ is found, its discrete counterpart can be constructed by initiating the construction algorithm with $w_{m,0} = r\phi_x(mr,0)$ and $w^*_{m,0} = r\phi_y(mr,0)$ for a small discretization step r.

4. Examples

Here, we exploit our results to describe how a few surfaces of interest, such as spheres and ruled surfaces, can or cannot be fitted.

4.1. Local fittings and spheres

Can any smooth surface be locally fitted by an eggbox? Locally, a smooth surface is characterized by its Gaussian curvature K and its mean curvature H. In the parametrization ϕ, these are given by

$$K = \frac{LN - M^2}{16s^2s^{*2}}, \qquad H = \frac{1}{2}\left(\frac{L}{4s^2} + \frac{N}{4s^{*2}}\right).$$

Thus, S can be locally fitted if and only if we can find real numbers (s, s^*, L, M, N) that yield K and H through the above equations while satisfying $(*)$.

A solution (s, s^*, L, M, N) can be constructed in the following manner. Letting

$$2A = \frac{L}{1-s^2} = \frac{N}{1-s^{*2}}, \qquad a = 16s^2s^{*2} > 0, \qquad b = \frac{1-s^2}{4s^2} + \frac{1-s^{*2}}{4s^{*2}} > 0,$$

the equations to solve simply become

$$K = \frac{A^2 - M^2}{a}, \qquad H = bA$$

and can be inverted into

$$A = \frac{H}{b}, \qquad M = \sqrt{\frac{H^2}{b^2} - aK}$$

as long as we can find a value of s such that $H^2/b^2 - aK \geq 0$, i.e., $1/(ab^2) \geq K/H^2$. Note that since K and H correspond to the determinant and half the trace of a symmetric matrix, the ratio K/H^2 is never larger than 1. Then, inspecting $1/(ab^2)$ as a function of s, by plotting it numerically for instance, it is

seen that it increases from 0, at $(s = 0, s^* = \sqrt{3}/2, \theta = 0)$, to 1, at $(s = \sqrt{2}/2, s^* = \sqrt{2}/2, \theta = \pi/2)$ and decreases back to 0, at $(s = \sqrt{3}/2, s^* = 0, \theta = 2\pi/3)$.

In conclusion, there are three scenarios.

- If $K/H^2 < 0$, i.e., for surfaces of negative Gaussian curvature, then any value $\theta \in]0, 2\pi/3[$ can achieve the local fitting.
- If $0 \leq K/H^2 < 1$, then there exists an interval of values $[\theta_1, \theta_2]$ any of which can achieve the local fitting. This interval shrinks as K/H^2 increases.
- If $K/H^2 = 1$, then there exists a unique value of θ that can achieve the local fitting, namely $\theta = \pi/2$.

Note that these fittings are local and are only valid in the immediate vicinity of a given point P of S. In other words, the fitting error will generally grow indefinitely as we move away from P. Even though we just proved that any smooth surface can be locally fitted by an eggbox, the existence of a global fitting, i.e., where the fitting error remains bounded and small across all of S, is a whole different story. In fact, a corollary to our discussion is that the eggbox cannot fit any finite region of a sphere for which $K/H^2 = 1$. To see why, recall that such a fitting requires θ be a constant equal to $\pi/2$. This implies that the metric is a constant and that Gaussian curvature is 0 clearly in violation of $K/H^2 = 1$.

4.2. Ruled surfaces

A rather simple method for fitting ruled surfaces can be derived by letting θ indefinitely approach 0:

$$\theta(x, y) = \delta\theta_0(x, y), \qquad \delta \to 0.$$

In that limit, s approaches 0 as well whereas s^* approaches $\sqrt{3}/2$. Thus, to avoid the appearance of a singular metric, we introduce a new coordinate system $X = x/\delta$, $Y = y$ so that, in the limit, the first and second fundamental forms become

$$I = \begin{bmatrix} 4s_0^2 & 0 \\ 0 & 3 \end{bmatrix}, \qquad II = \begin{bmatrix} L_0 & M_0 \\ M_0 & 0 \end{bmatrix}.$$

These fundamental forms describe exactly all ruled surfaces. Note that ϕ_Y which is aligned with ϕ_y is in the direction of the generatrix whereas ϕ_X, parallel to ϕ_x, is orthogonal to the generatrix.

As an example, we construct the fitting of a one-sheeted hyperboloid S, say that of equation $z_3^2 + 1 = z_1^2 + z_2^2$, $(z_1, z_2, z_3) \in \mathbb{R}^3$. In a first step, we look for a curve $\Psi(x)$ that belongs to S and is orthogonal to the generatrix at all of its points. One such a curve is

$$\Psi(x) = \frac{1}{2}(x\cos x - 2\sin x\,, x\sin x + 2\cos x\,, x\,).$$

The corresponding tangent vectors aligned with Ψ and the generatrix respectively are

$$W(x) = \frac{1}{2}(-x\sin x - \cos x\,, -\sin x + x\cos x\,, 1), \qquad W^*(x) = \frac{1}{\sqrt{2}}(\cos x\,, \sin x\,, 1).$$

In a second step, we re-parametrize path Ψ using a small parameter α in the spirit of the asymptotics presented above for ruled surfaces. Thus, we let

$$\psi(x) = \Psi(\alpha x), \qquad w(x) = \alpha W(\alpha x), \qquad w^*(x) = 2s^* W^*(\alpha x),$$

with $s = \|w\|/2$ and $s^* = s^*(s)$ as always. Third, let r be the edge size of the fitting pyramids chosen small compared to the typical radius of curvature of S, say $r = 0.1$. In the fourth and last step, we initialize our construction algorithm with the initial data $w_{m,0} = rw(mr)$ and $w^*_{m,0} = rw^*(mr)$, for m spanning the integers between 0 and $2\pi/(\alpha r)$.

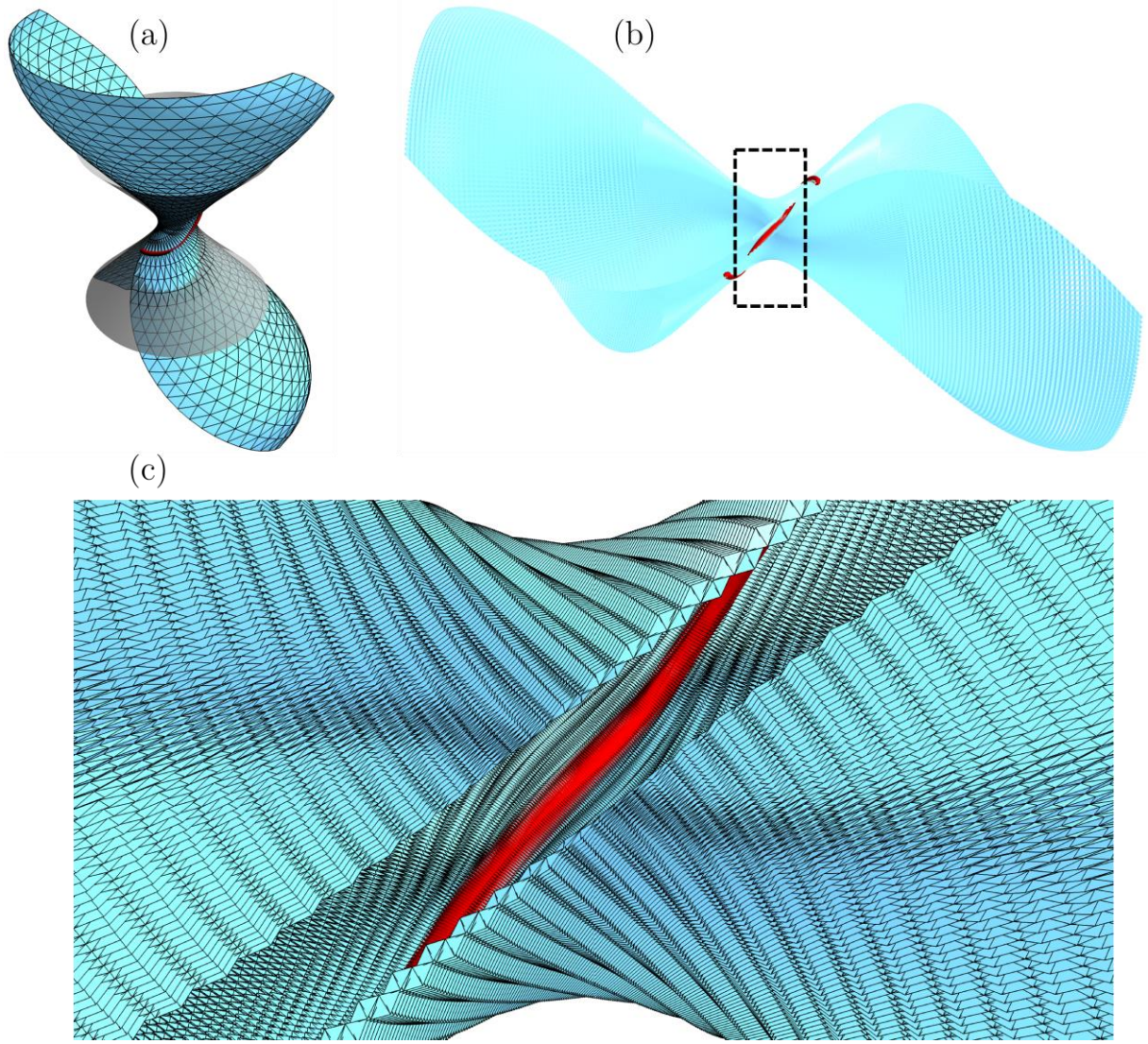

Figure 5: Fitting of a one-sheeted hyperboloid: (a) the target hyperboloid is in gray and the fitting's mean surface (pyramids bases only) is in blue; (b) the fitting with unmarked edges; (c) a closeup look at the region surrounded by a dashed rectangle in (b) with edges marked in black. Edges belonging to the diagonal D_0 with which the algorithm was initiated are highlighted in red.

The resulting fitting is shown on Figure 5 for $\alpha = 0.2$ and $x \in [-\pi/\alpha, \pi/\alpha]$ so that all generatrices are spanned. Improving the quality of the fitting requires considering smaller values of r and of α whereas extending it requires taking larger x intervals.

5. Conclusion

It is of interest to study other pin-jointed trusses and origami tessellations using the theory exemplified here. It turns out that Nexorades [5] as well as Ron Resch patterns [9,11] may only fit developable surfaces asymptotically. The method could benefit from improvements especially by taking boundary layers into account. These develop over length scales comparable to the unit cell parameter and thus necessarily escape the present approach. The importance of boundary layers in describing the kinematics of origami tessellations is perhaps best understood through the example of the Ron Resch pattern: it can only fit developable surfaces in the homogenization limit and yet can acquire significant positive

curvatures through large deformations that initialize on the boundaries of any finite sample and remain localized at the unit cell scale.

References

[1] Ciarlet PG. An Introduction to Differential Geometry with Applications to Elasticity. *J Elast* 2005;**78**–**79**:1–215.

[2] Douthe C, Baverel O, Caron J-F. Gridshell in composite materials: Towards wide span shelters. *J Int Assoc Shell Spat Struct* 2007;**48**:175–80.

[3] Euler L. De Solidis quorum superficiem in planum explicare licet. *Novi Coment Acad Sci Imp Petropolitanae*, 1772;**XVI**:3–34.

[4] Ghys É. Sur la coupe des vêtements. Variation autour d'un thème de Tchebychev. *L'Enseignement Mathématique* 2011;**57**:165–208.

[5] Greco L, Lebée A, Douthe C. Investigation of the elastic behavior of reciprocal systems using homogenization techniques. *Proc Int Assoc Shell Spat Struct Symp* 2013.

[6] Hochfeld H. Process and Machine for Pleating pliable materials, 1959.

[7] Miura K. Method of Packaging and Deployment of Large Membranes in Space. *ISAS Rep* 1985.

[8] Nassar H, Lebée A, Monasse L. Curvature, metric and parametrization of origami tessellations: theory and application to the eggbox pattern. *Proc R Soc A* 2017;**473**:20160705.

[9] Resch RD, Christiansen H. The design and analysis of kinematic folded-plate systems. Proc. Symp. folded plates Prism. Struct. Int. Assoc. shell Struct., Vienna: 1970.

[10] Schenk M, Guest SD. Origami folding: A structural engineering approach. In: Wang-Iverson P, Lang RJ, YIM M, editors. Origami 5 Fifth Int. Meet. Origami Sci. Math. Educ., 2011, p. 1–16.

[11] Tachi T. Designing Freeform Origami Tessellations by Generalizing Resch's Patterns. *J Mech Des* 2013;**135**:111006.